buildings

MDPI

Review

A Review of Large-Eddy Simulation Cell Size Requirements for Indoor Flows

Ferenc Szodrai

Department of Building Services and Building Engineering, Faculty of Engineering, University of Debrecen, 4028 Debrecen, Hungary; szodrai@eng.unideb.hu

Abstract: Nowadays computational fluid dynamics now assists ventilation system designers and architects in understanding the induced flow behaviour in the indoor environment. The use of large-eddy simulation is a novel methodology for these types of assessments. The method requires that the computational domain be adequately discretized in order to resolve the majority of the flow. The last five years of publications of Elsevier, SAGE, and Multidisciplinary Digital Publishing Institute were screened. Indoor flow categories were utilized to assess the differences. Based on the papers reviewed, the cell size requirement was considered as a key factor of computational demand. Specifications were made for each type of indoor flow simulation.

Keywords: indoor flow; natural ventilation; mechanical ventilation; large-eddy simulation; dispersion; thermal comfort; mesh size; mesh quality

Citation: Szodrai, F. A Review of Large-Eddy Simulation Cell Size Requirements for Indoor Flows. *Buildings* **2023**, *13*, 2159. https://doi.org/10.3390/buildings13092159

Academic Editor: Ricardo M. S. F. Almeida

Received: 1 August 2023
Revised: 22 August 2023
Accepted: 23 August 2023
Published: 25 August 2023

1. Introduction

Analysis of indoor air quality is a well-studied and frequently researched topic; many review articles also highlight that it has many relevant sub-levels, both in measurement [1–3] and in computational fluid modelling [1,3–7].

As most human activity nowadays takes place indoors, it is critical to have adequate indoor air quality (IAQ) [1,8,9]. A room with adequate IAQ can provide adequate thermal comfort, has low levels of air pollution or contaminants, and has no draughts. Indoor air flow can have an effect on all of the factors influencing IAQ. Indoor flow can be induced in a building in a variety of ways, such as by opening the windows and letting breeze flow through the building, but airing the room must be performed with caution due to the fact that high velocities [10] should not be allowed in most cases [11]. Airing the room could also have other disadvantages, such as the uncontrolled air quality and quantity which should not be preferred in environments where the comfort requirements are high. As a result, mechanical ventilation systems are mostly preferred, due to their better control over the flow structures. Mechanical ventilation has two common designs: mixing and displacement ventilation. With mixing ventilation (MV) the aim is to mix the fresh air into the domain, while displacement ventilation (DV) aims to "push out" the used air with the help of fresh air. These kinds of mechanical ventilation systems could create different flow structures in the examined area [12,13]. The key question about these ventilation methods is always: how much used or contaminated air can be extracted from the room with the least amount of fresh air? For a long time, the decisions of designers were based on previous experience. Nowadays, as the availability of complex simulations is growing, designers can create scenarios for their current work to evaluate or strengthen their inspirations, or simply use a research paper that can provide a helpful idea to begin the design process.

With computational fluid dynamics (CFD) and by using some governing equations, a digital model of the indoor environment can be created, in which flow patterns, velocity fluctuations, or the movement of a pollutant can be tracked in isothermal or non-isothermal scenarios.

There are two approaches to using CFD simulations to describe an indoor flow: the most common one is to use a steady or unsteady Reynolds-averaged Navier–Stokes

(RANS or URANS) simulation, and the other one is large-eddy simulation (LES). The RANS and URANS methods are widely used because they produce accurate and quick results with low computational cost, and, furthermore, give researchers safety since it is a commonly used method. Even in novel studies [14–17] RANS methods are still favoured.

While the LES method requires significantly more computational power [18], URANS counterparts can be similarly accurate to some extent. This fact was investigated in numerous papers where RANS and LES numerical [19,20], and experimental [21] results were compared. The similarity of the flows was consistent but, as Zhang et al. [22] demonstrated, the fine vortex formations did not appear in the RANS version of a cross-ventilated room. Furthermore, when Auvinen et al. [23] examined pollutant risk reduction methods, the accuracy of LES was more reliable than that of other methods.

The reason for this is that, with RANS, the small-scale velocity fluctuations are modelled, while LES resolves the majority of them and the rest is filtered. For a relatively smaller environment with complex flow patterns, LES would be a suitable option [24]. A detailed comparison of RANS and LES has been made by Blocken [25] for indoor flow modelling to have a clear view of the main differences in general.

This review focuses on the computational demands of the LES method for indoor flows to provide additional guidance when deciding for RANS or LES. To oversimplify the computational demand, the examined domain should be sliced into sufficiently small volumes and the unsteady process should be sliced into sufficiently small time steps. These two variables largely determine the computational requirements and time. The former was investigated, whereas the latter received less attention because it is dependent on additional external effects that cannot be considered uniformly. For example, airflow covers a greater distance in a large indoor area [26] than in a closed laboratory room [27]. Of course, adding thermal or particle movement governing equations can make the model more challenging.

Thus, the task was to collect and assess indoor flow-related, large-eddy simulation studies from the previous five years. The limitation of this study is that it does not deal with adjacent research areas such as atmospheric boundary layer assessments of urban regions or sole evaluations of air terminal units or any other part of a ventilation system using the LES method.

2. Materials and Methods

For this assessment, research and review papers were collected from the beginning of 2018 to June 2023, from the Elsevier, SAGE, and MDPI (Multidisciplinary Digital Publishing Institute) databases using the keywords: indoor, ventilation, and large-eddy simulation. Keywords could be found in the title, abstract, or keywords. In total, 182 publications were screened, 73 were mentioned, and 37 were used for the evaluation. Conference papers and irrelevant works were excluded; the pivotal papers in the field, as well as relevant references in research papers, were additionally included. Figures from research papers are intentionally not presented.

The review evaluates the applicability of the LES method for indoor flows, specifically its discretization requirement (e.g., the cell size), accuracies, and model purposes. It would also highlight the flaws and potential new research areas associated with this method.

3. Results

Each year, the terms “large-eddy simulation” or “indoor” generated thousands of publications, according to Web of Science data demonstrating that these fields are relevant and well-studied. Surprisingly, when the two keywords were searched together, only a fraction of the amount was revealed. So far, an average of fifteen to twenty publications have been produced per year; see Figure 1 for additional distributions. The trend is increasing steadily; additionally, it suggests that the field may have potential.

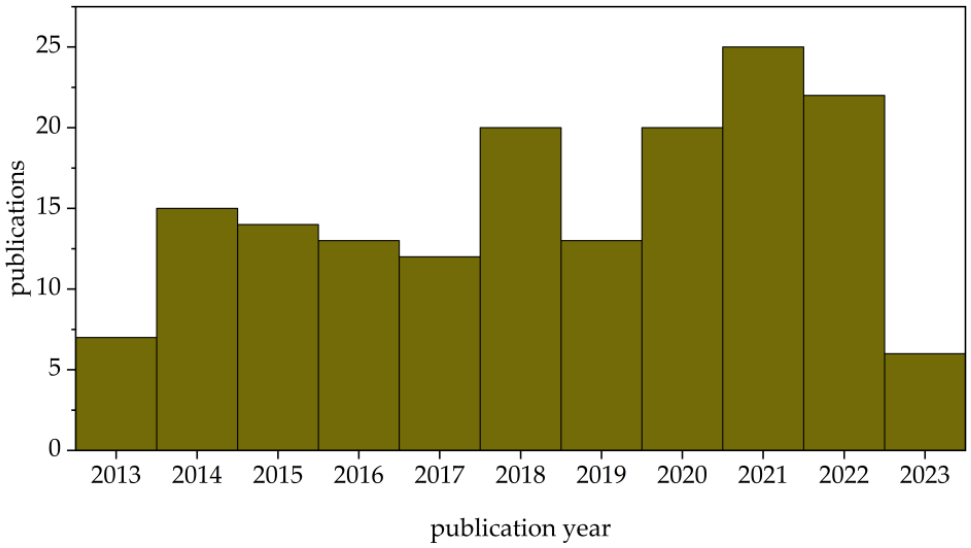

Figure 1. Publication distribution over the years for indoor and large-eddy simulation studies.

The reason for the steady increase could be that graphics processing units [28,29] and high-performance computing are becoming more and more available.

3.1. Cell Size

In a CFD model after defining the geometry of the computational domain, the meshing has to be created and, when it is carried out for the discretized points, the governing equations are calculated. That is why it is relevant to know that, when a coarse mesh is used, it might affect the results of the model and, when a fine mesh is, the accuracy does not decrease but the computational demand can reach the computational capacity. Typically, the number of the used cells is determined by a grid convergence index (GCI) developed by Roache [30]. By using three different meshing sizes, one can determine whether the mesh is influenced by the computational grid. The cells in LES have high-quality demand; thus, hexahedral cells are favoured since the structured mesh has excellent mesh quality in the free-flow zone (outside the boundary layer). At the near-wall zone, other unstructured types of cell geometries are required to describe the domain. On the surfaces ten to twenty prismatic cells are applied, which are usually shorter than the hexahedral cells. The first layer height is defined by a non-dimensional number, y^+, which is calculated by a CFD software, and it should be below one to get accurate results. The upper limitations of y^+ could also be exceeded by choosing different kinds of simulation methods but even with hybrid RANS-LES models [31] the value was kept below. The upper cells are allowed to be larger; however, the growth rate should be revised and keep in mind that between the prismatic and hexahedral meshes the transitional cells could have low quality.

3.2. Types of Research

Only publications from the last five years were examined. The screened publications revealed three major types of simulations. In "Natural Flow Type" (NFT), wind tunnel assessments were made to examine wind-induced, natural ventilation flow patterns through certain buildings. The "Dispersion Flow Type" (DFT) publication assesses particle dispersion in indoor environments. Publications of the "Thermal Flow Type" (TFT) assess ventilation effectiveness by simulating buoyancy influenced airflow patterns.

Figure 2 represents a sketch of the mentioned three main types of studies; overlapping between categories could occur; however, these are the three main flow types in the study.

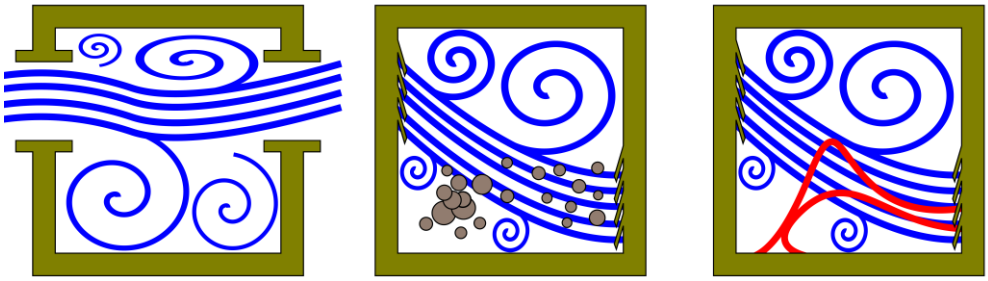

(**a**) (**b**) (**c**)

Figure 2. The sketch for the three types of studies. NFT (**a**); DFT (**b**); TFT (**c**). (Green: building; blue: stream lines; grey: particles; red: heat).

3.3. Sub-Grid Quality Indicators

RANS employs various turbulence models [32,33], whereas LES utilizes sub-grid scale models to resolve the stress tensor $|\bar{S}|$ [34], from which the sub-grid scale eddy viscosity (ν_{SGS}) can be calculated. The distinction between the various types of sub-grid models will be made here.

With a few exceptions, the studies under consideration share many characteristics. The Wall-Adapting Local Eddy-viscosity Model LES (WALE-LES) was used in most cases, except one research group that preferred the Wall Modelled LES (WM-LES) [21,35–38].

The WALE-LES model computes sub-grid scale eddy viscosity (ν_{SGS}) as follows:

$$\nu_{SGS} = (C_W \cdot \Delta)^2 \cdot |\bar{S}| \quad (1)$$

where C_W is a constant for this method between 0.3–0.6 [39] and Δ is the filter length or cell size. This model requires slightly less computational power than its predecessors. It is also accurate at near-wall flow; the only downside of it is that fine meshing is required; thus, it would be pivotal to know the recommended cell size.

Another quality indicator for cell size could be the Courant–Friedrichs–Lewy (CFL) condition [40]. It is a stability condition for unsteady flows, which is expressed as follows:

$$CFL = v \cdot \Delta t / \Delta < 1 \quad (2)$$

where v is the magnitude of the velocity at the cell, Δt is the time step size, and Δ is the cell size.

Now, it is clear that Δ is important for the LES method and, because the velocity regime is typically low in an indoor environment ($v_{max} \approx 1$ m/s even when some requirement level is exceeded), the time step and cell size may exhibit some uniform characteristics.

When the cell size is established, the size of the time step could be determined by maintaining the CFL condition. According to the screened papers, the time step is usually a fraction of a millisecond [22,41].

Before dealing with the total duration of the simulation, the flow-through time should be mentioned. This flow-through duration demonstrates how long it takes to move along the indoor environment at a given velocity. Typically, for naturally ventilated and dispersed particle tracking cases, a simulation should investigate 24–30 flow-through times no matter the size of the indoor environment. As demonstrated by Thysen et al. [42], a simulation with 28 flow-through times and 1 ms time step duration divided the simulation into a quarter million time steps. These parameters correspond to another review for internal flows [43]. Thermal related studies can be less computationally expensive, with a significantly lower total number of time steps [44].

3.4. Attained Dimensions

As the average Δ is rarely stated on paper, some calculation is required, resulting in minor inaccuracies when determined.

The mesh density is the ratio of the number of cells (which is the product of the mesh sensitivity analysis) to the volume of the computational domain. Then, since most meshes have a hexahedral shape, the cubic root of the cell volume can give an average cell size. This value includes the inaccuracy due to the size difference between the boundary layer and the transitional unstructured mesh. It is worth noting that only one study used unstructured mesh [45] and it is usually used for RANS. The level of inaccuracies is around one digit between the free flow cell size and the average cell size. When the boundary layer is so small that the experimental measurement cannot depict it, the near-wall zones can be thoroughly analysed using CFD, as demonstrated by Bazdidi-Tehrani et al. [46].

3.4.1. Natural Flow Type Studies

In an indoor environment natural flow occurs when due to the opened building envelope the wind might blow through its hollow structure. As Xiao et al. [47] summarized, the wind has turbulent behaviour and it is affected by the buildings around the domain in scope. Both direction and magnitude may fluctuate in time, which makes it difficult to add a boundary condition for a naturally ventilated room. That is why in these studies the building is placed in a wind tunnel (see Figure 2a). The scale of the open area could vary from a small enclosure [26] through a repetitive pattern [7,48,49] to a section of a city [50,51].

This category is often limited to assess solely the natural flow since the induced mechanical ventilation, or buoyant flow, could only slightly alter the main flow structure. Another common feature was that the examined rooms were hollow [41,52,53] and they had no obstacles in them. Multiple zones were considered to be unique [54,55].

The limitations of these studies arise from the need to describe the movement of the atmospheric boundary layer (ABL). The reason for this is that buildings are located in the viscous sublayer of the ABL, where LES typically predicts the velocity distribution less accurately. Furthermore, the prismatic layers that are commonly used in CFD simulations are not always present in an indoor environment. Hooff et al. [56] demonstrated that near-wall flows were less relevant, which could reduce inaccuracies. When compared to wind tunnel measurements, it is clear that the boundary layer of the indoor flow had no significant effect on the speeds.

The NFT subcategory could be represented by the work of Zhang et al. [53], where the wind flow created various kinds of indoor flow patterns based on where the openings were placed. In addition, the aim can be a combination of subcategories as in Bazdidi-Tehrani et al. [46], where the pollutant removal capabilities of the natural flow were assessed and a thermal comfort calculation could be performed which was showcased by Hirose et al. [10].

With a few exceptions, the mentioned paper only investigated ventilation effectiveness. Hirose et al. [7,10] conducted a thermal analysis of naturally ventilated rooms. It can also be seen that, when an additional thermal model is used, this helps only a little to gain better accuracy when compared to a similar study by Adachi et al. [52]. Laetitia et al. [55] conducted an additional assessment by combining the LES model with a zero-dimensional building energetic model.

The Δ is typically less than 50 mm (see Table 1) but it can be as low as 1 mm depending on the size of the domain, which necessitates minimal computational demand. However, when the scale is robust, the Δ can reach 1 m, as demonstrated by Hwang et al. [50], who created an urban scale model to evaluate a single room.

Table 1. NFT studies.

Authors	Cell Size (mm)	Ventilation Type	Room Type
Zhang et al. [53]	6.6	NV	SR with doors
Carrilho da Graça et al. [41]	43.7	NV	SR (corner office)
Hwang et al. [50]	1289.2	NV	SR
Hirose et al. [7,10]	1	NV	SR is modelled using a block array
Adachi et al. [52]	10	NV	
Laetitia et al. [55]	28.8	NV	Multiple room
Bazdidi-Tehrani et al. [46]	13.9	NV	SR
Zhang et al. [22]	42.5	NV	SR
Arinami et al. [49]	18.2	NV	SR with various orientations and guide vanes
Dai et al. [48]	5	NV	
Hawendi et al. [54]	1.5	NV	Multiple rooms

NV: natural ventilation, SR: single room.

3.4.2. Dispersion Flow Type Studies

Indoor flow research has two distinctive aims, one of which examines the particle dispersions, focusing on how a certain particle type contamination threat can be reduced (DFT), and the other one focuses more on the influence of buoyant flow (TFT). The dispersed particle can be anything; nowadays viruses [57,58] are more common; however, they could also be combustion products [59].

Figure 2b shows that, in the DFT studies, there is a specific type of pollutant source in the domain that could contaminate other residents with the indoor flow. As a result of these studies, the HVAC designer should be able to select and place the most favourable air terminal unit in the room [8].

In these DFT works, the particle transport prediction mechanism varied from Lagrangian and LES coupled model [45] to the Multi Relaxation Time Lattice Boltzmann Method [44], also a combination of fast fluid dynamics and a Markov chain model, which was validated by LES [60]. Because the small particles must be accurately described, this method is computationally intensive. Li et al. [61] demonstrated that these types of LES models give good agreement with particle image velocimetry measurements.

Usually, the contaminated flow is situated outside of the boundary layer; thus, it makes the LES method an accurate tool.

From Table 2 it can be concluded that isothermal mixing ventilation Δ is usually around 30–40 mm and it only becomes finer when a coupled model, such as a rotating ceiling fan [61], is also added to the system or buoyant flow is present [23].

Table 2. DFT studies.

Author	Cell Size (mm)	Ventilation Type	Room Type
Zheng et al. [62]	26.4	Door opening and MV	Hospital rooms
Li et al. [61]	19.2	Ceiling fan and MV	M
Chu et al. [63]	10.3	NV	Garage
Laitinen et al. [64]	25–6.25	MV	M
Thysen et al. [42]	6.3	DV	M
Auvinen et al. [23] & Oksanen et al. [57]	8.4	DV with buoyant flow	Restaurant
Salinas et al. [3]	29.7	MV	SR
Li et al. [12]	79.4	MV + DV	SR with obstacles
Sajjadi et al. [44]	79.4	MV	SR
Vuorien et al. [58]	25	MV	M
Feng et al. [65]	24	Buoyant flow	M
Liu et al. [60]	42.5	MV	Two rooms
Hooff et al. [19]	36.2	MV	SR
Zhang et al. [45]	38.9	MV	M
Kosutova et al. [20]	31.2	MV	SR

NV: natural ventilation, MV: mixing ventilation, DV: displacement ventilation, SR: single room, M: manikin(s) in a single room.

In contrast to NFT, these studies used manikins to create obstacles in the indoor environment. Their goals were to create a more realistic flow pattern.

Interestingly, these types of studies focus solely on the mixing ventilation-caused flow patterns, which impact the near-wall flow less.

3.4.3. Thermal Flow Type Studies

In a ventilated and in a non-ventilated room, the air flow patterns and velocity magnitudes could be significantly different due to the thermal plume effect [13,66]. The thermal plume is the result of the buoyant flow which is caused by the temperature difference between the surface and the air. This flow structure could easily be obliterated even with a slight breeze. In a complex environment many heat sources are present [65] and even fire could occur [67,68].

Studies of this category in the last five years were rare, which has two reasons. The buoyant flow often coupled with external flow [23,57,63,65] and the RANS method is still favoured as it was mentioned previously.

This category was assumed to have the highest computational demand by default because the thermal convection around the examined area must be accurately described. This is because the y^+ for the thermal boundary layer should be even smaller. The experimental values did not show but the numerical model showed the signs of boundary layers in the work of Hurnik et al. [21], where a jet flow was assessed in a room. The cell count of their LES model had to be doubled to have independent and acceptable results when a non-isothermal model was utilized.

From the screened LES papers, the smallest Δ used for the TFT studies (see Table 3) could be attributed to the small volume and the coupled thermal model. Also, these types of studies turned out to be nowadays the rarest.

Table 3. TFT studies.

Author	Cell Size (mm)	Ventilation Type	Room Type
Fang et al. [67]	100	Buoyant	SR
Huang et al. [68]	183	Buoyant	SR
Hurnik et al. [21]	6.4	SWJ	SR
Larkermani et al. [69]	12.2	Buoyant	Between a cold and a warm room
Zasimova et al. [37] and Ivanov et al. [35,36,38]	11.9	SWJ	SR
Taghinia et al. [27]	19.3	SWJ	M

SWJ: sidewall jet, SR: single room, M: a manikin in a single room.

3.4.4. Comparison

The applied cell sizes from Tables 1–3 are summed up in Figure 3 to compare the categories; because there are few peaking scenarios on Figure 3, they are intentionally not depicted but they are included in the statistical analysis.

So as to give a recommendation for mesh size, it would be relevant to know what we should take into account. Firstly, the mean value of the screened studies could be misleading due to the peaking studies [50,67,68], since the mean values of cell size of the categories were: $\Delta_{meanNFT}$ = 132 mm, $\Delta_{meanDFT}$ = 29 mm, and $\Delta_{meanTFT}$ = 38 mm. However, the 25% and 75% quartile values for the categories were $\Delta_{quartileNFT}$ = 5–42.5 mm, $\Delta_{quartileDFT}$ = 10.3–36.2 mm, and $\Delta_{quartileTFT}$ = 11.9–19.3 mm. Excluding the peaking scenarios would cause the mean value and the median value to become closer to each other and the mean value would be in the quartile range.

The cell sizes are close to each other when using median values of $\Delta_{meadianNFT}$ = 13.9 mm, $\Delta_{meadianDFT}$ = 25 mm, and $\Delta_{meadianTFT}$ = 11.9 mm. In general, for any indoor-LES-related model the cell size should be less than 40 mm; furthermore, researchers should aim for Δ = 10 mm. Now that a recommendation is known, it would be useful to know how

many cells are used. Larkermani et al. [69] had the highest cell count with 127 million and the domain was 233 m^3. The average cell count in the studies was less than 5 million. The mentioned mesh size is achievable nowadays even with a desktop computer. It is also notable that the minimum cell size was above 6 mm which could help the reader not to choose too fine a mesh. By selecting arbitrarily from RANS studies two could be mentioned, one that uses cell size close to the 75% quartile Δ = 33 mm [70] and another one, which has a significantly smaller cell size in the domain Δ = 0.08 mm [71]. Yet for large-scale Direct Numerical Simulation (DNS) Δ = 3.15 mm [72] was used, which is fine for LES, though for DNS it could be coarse similarly to a two-dimensional flow study with Δ = 18 mm [73].

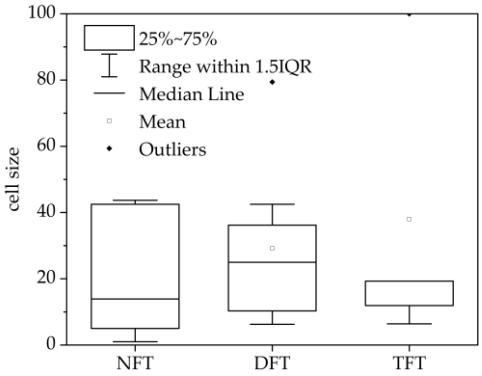

Figure 3. Average cell length in different types of studies (NFT: Natural Flow Type; DFT: Dispersion Flow Type; TFT: Thermal Flow Type; IQR: quartile range).

4. Conclusions

A systematic review of indoor flow-related research using the large-eddy simulation method was conducted. The screened studies identified three types of flow, Dispersion Flow Type, Natural Flow Type, and Thermal Flow Type pattern. All of them served different purposes and differed primarily in whether an external domain was added or additional tasks were completed. It should be noted that the indoor flow analysis does not include ventilation duct, air handling unit, or air terminal unit flow analysis. The aim was to establish a recommended cell size range for indoor flows, while the length of the calculation time still remained open, since more complex methods or geometries could extend the duration of the solver process. Based on the screened papers the following conclusions were made:

- The large-eddy simulation is now a more suitable tool for assessing a more detailed flow pattern than RANS. From an architectural standpoint, LES cross-ventilation can be designed and its accuracy has been demonstrated by experimental data. It also has the potential to assess the effectiveness of mechanical ventilation when pollutant levels are high in the indoor environment.
- The screened papers show that in the scope of indoor flow the topic of simulation with LES particle dispersion is more frequent than thermal flow related topics.
- One of the limitations of the study is its scope. It heavily focuses on indoor LES research, on which only a few articles have been published in recent years. This could be explained by the high computational demand and scarcity of the LES method application. RANS is preferred with relatively coarser mesh and lower computational capacity, making researchers biased when selecting flow description methods.
- Many RANS studies could have been conducted using the same computational grid and the LES method. This observation is also supported by the fact that many of the studies examined focus on comparing LES with RANS and conclude that only minor differences exist.
- The studies focused on the cell size of the used mesh in LES studies and it was confirmed that fine meshing was required, which means that a higher load on the memory was required. Another requirement that was only marginally taken into account was

the number of time steps required to consider a model to be calculated. GPU-based solvers provide hope for reducing the difficulties caused by simulation length.

- All papers included in the cell size evaluation were compared to experimental studies and found to be in good agreement. The calculation in the viscous sublayer is still regarded as difficult but the WALE-LES method handled it well. More and more dispersion-related research showed that more and more accurate methods were being developed, proving that the previous, less computationally demanding, methods were also less accurate.
- The element size could vary regardless of the size of the dispersed particle.
- Larger element sizes were allowed because the viscous sublayer had little influence on the main free flow structure.
- The maximum recommended cell size became 40 mm and the minimum became 10 mm.
- If the model calculated particle dispersion or thermal convection in the flow, the lower limit should be used.
- The upper limit can be used for isothermal flow pattern assessment.

To mention a potential under-researched field, purely thermal and flow-related problems are unique, with only a few studies using LES in the last few years. This could be due to the flaws mentioned earlier. However, because the created flow patterns can be more accurately described around the manikins or humans in the tested rooms, it may be a relevant field in thermal comfort assessment.

Funding: Project no. TKP2021-NKTA-34 has been implemented with support provided by the National Research, Development and Innovation Fund of Hungary, financed under the TKP2021-NKTA funding scheme.

Conflicts of Interest: The author declares no conflict of interest.

References

1. Argyropoulos, C.D.; Skoulou, V.; Efthimiou, G.; Michopoulos, A.K. Airborne transmission of biological agents within the indoor built environment: A multidisciplinary review. *Air Qual. Atmos. Health* **2023**, *16*, 477–533. [CrossRef] [PubMed]
2. Nielsen, P.V.; Xu, C. Multiple airflow patterns in human microenvironment and the influence on short-distance airborne cross-infection—A review. *Indoor Built Environ.* **2022**, *31*, 1161–1175. [CrossRef]
3. Salinas, J.S.; Krishnaprasad, K.A.; Zgheib, N.; Balachandar, S. Improved guidelines of indoor airborne transmission taking into account departure from the well-mixed assumption. *Phys. Rev. Fluids* **2022**, *7*, 064309. [CrossRef]
4. Mesenhöller, E.; Vennemann, P.; Hussong, J. Unsteady room ventilation—A review. *Build. Environ.* **2020**, *169*, 106595. [CrossRef]
5. Toparlar, Y.; Blocken, B.; Maiheu, B.; van Heijst, G.J.F. A review on the CFD analysis of urban microclimate. *Renew. Sustain. Energy Rev.* **2017**, *80*, 1613–1640. [CrossRef]
6. Tsang, T.-W.; Mui, K.-W.; Wong, L.-T. Computational Fluid Dynamics (CFD) studies on airborne transmission in hospitals: A review on the research approaches and the challenges. *J. Build. Eng.* **2023**, *63*, 105533. [CrossRef]
7. Hirose, C.; Ikegaya, N.; Hagishima, A.; Tanimoto, J. Computational fluid dynamics for cross-ventilated airflow in a urban building. *Jpn. Archit. Rev.* **2022**, *6*, e12312. [CrossRef]
8. Szekeres, S.; Kostyák, A.; Szodrai, F.; Csáky, I. Investigation of Ventilation Systems to Improve Air Quality in the Occupied Zone in Office Buildings. *Buildings* **2022**, *12*, 493. [CrossRef]
9. Qiu, Y.; Wang, Y.; Tang, Y. Investigation of indoor air quality in six office buildings in Chengdu, China based on field measurements. *Build. Simul.* **2020**, *13*, 1009–1020. [CrossRef]
10. Hirose, C.; Ikegaya, N.; Hagishima, A.; Tanimoto, J. Indoor airflow and thermal comfort in a cross-ventilated building within an urban-like block array using large-eddy simulations. *Build. Environ.* **2021**, *196*, 107811. [CrossRef]
11. *PD CR 1752:1999*; Ventilation for Buildings—Design Criteria for the Indoor Environment. European Committee for Standardization: Brussels, Belgium, 1998.
12. Li, C.; Zhao, Y.; He, Y.; Luo, K.H.; Li, Y. Simulation of indoor harmful gas dispersion and airflow using three-dimensional lattice Boltzmann method based large-eddy simulation. *AIP Adv.* **2021**, *11*, 035235. [CrossRef]
13. Kalmár, T.; Szodrai, F.; Kalmár, F. Local ventilation effectiveness dependence on the airflow pattern and temperature in the case of isothermal balanced ventilation. *J. Build. Eng.* **2022**, *61*, 105309. [CrossRef]
14. Jeong, D.; Yi, H.; Park, J.H.; Park, H.W.; Park, K.H. A vertical laminar airflow system to prevent aerosol transmission of SARS-CoV-2 in building space: Computational fluid dynamics (CFD) and experimental approach. *Indoor Built Environ.* **2022**, *31*, 1319–1338. [CrossRef]

15. Meng, C.; Liu, D.; Gao, N.; Li, L. Investigation on improving fume hood performance via elimination of internal vortices: Experiments and CFD. *Indoor Built Environ.* **2022**, *31*, 2467–2481. [CrossRef]
16. Wang, C.; Zhang, J.; Chao, J.; Yang, C.; Chen, H. Evaluation of dynamic airflow structures in a single-aisle aircraft cabin mockup based on numerical simulation. *Indoor Built Environ.* **2022**, *31*, 398–413. [CrossRef]
17. Fan, Y. A TOPSIS optimization for the indoor thermal environment through oscillating airflow generated from a cassette split type air conditioner. *Indoor Built Environ.* **2021**, *30*, 1200–1210. [CrossRef]
18. Morozova, N.; Trias, F.X.; Capdevila, R.; Pérez-Segarra, C.D.; Oliva, A. On the feasibility of affordable high-fidelity CFD simulations for indoor environment design and control. *Build. Environ.* **2020**, *184*, 107144. [CrossRef]
19. van Hooff, T.; Blocken, B. Mixing ventilation driven by two oppositely located supply jets with a time-periodic supply velocity: A numerical analysis using computational fluid dynamics. *Indoor Built Environ.* **2020**, *29*, 603–620. [CrossRef]
20. Kosutova, K.; van Hooff, T.; Blocken, B. CFD simulation of non-isothermal mixing ventilation in a generic enclosure: Impact of computational and physical parameters. *Int. J. Therm. Sci.* **2018**, *129*, 343–357. [CrossRef]
21. Hurnik, M.; Ivanov, N.; Zasimova, M.; Popiolek, Z. Local and gross parameters of air distribution in a room with a sidewall jet: CFD validation based on benchmark test. *Build. Environ.* **2022**, *207*, 108509. [CrossRef]
22. Zhang, X.; Weerasuriya, A.U.; Tse, K.T. CFD simulation of natural ventilation of a generic building in various incident wind directions: Comparison of turbulence modelling, evaluation methods, and ventilation mechanisms. *Energy Build.* **2020**, *229*, 110516. [CrossRef]
23. Auvinen, M.; Kuula, J.; Grönholm, T.; Sühring, M.; Hellsten, A. High-resolution large-eddy simulation of indoor turbulence and its effect on airborne transmission of respiratory pathogens—Model validation and infection probability analysis. *Phys. Fluids* **2022**, *34*, 076495. [CrossRef] [PubMed]
24. Cao, S.J. Challenges of using CFD simulation for the design and online control of ventilation systems. *Indoor Built Environ.* **2019**, *28*, 3–6. [CrossRef]
25. Blocken, B. LES over RANS in building simulation for outdoor and indoor applications: A foregone conclusion? *Build. Simul.* **2018**, *11*, 821–870. [CrossRef]
26. Chew, L.W.; Chen, C.; Gorlé, C. Improving thermal model predictions for naturally ventilated buildings using large eddy simulations. *Build. Environ.* **2022**, *220*, 109241. [CrossRef]
27. Taghinia, J.H.; Rahman, M.M.; Lu, X. Effects of different CFD modeling approaches and simplification of shape on prediction of flow field around manikin. *Energy Build.* **2018**, *170*, 47–60. [CrossRef]
28. Bieringer, P.E.; Piña, A.J.; Lorenzetti, D.M.; Jonker, H.J.; Sohn, M.D.; Annunzio, A.J.; Fry, R.N., Jr. A Graphics Processing Unit (GPU) Approach to Large Eddy Simulation (LES) for Transport and Contaminant Dispersion. *Atmosphere* **2021**, *12*, 890. [CrossRef]
29. Haque, M.J.; Molla, M.M.; Khan, M.A.I.; Ahsan, K. Graphics process unit accelerated lattice Boltzmann simulation of indoor air flow: Effects of sub-grid scale model in large-eddy simulation. *Proc. Inst. Mech. Eng. Part C J. Mech. Eng. Sci.* **2020**, *234*, 4024–4040. [CrossRef]
30. Roache, P.J. Perspective: A method for uniform reporting of grid refinement studies. *J. Fluid Eng.* **1994**, *116*, 405–413. [CrossRef]
31. Taghinia, J.; Rahman, M.M.; Siikonen, T. Numerical simulation of airflow and temperature fields around an occupant in indoor environment. *Energy Build.* **2015**, *104*, 199–207. [CrossRef]
32. Menter, F.R.; Lechner, R.; Matyushenko, A. *Best Practice: Generalized k-w Two-Equation Turbulence Model in ANSYS CFD (GEKO)*; ANSYS Germany GmbH: Darmstadt, Germany, 2019; pp. 1–38.
33. Menter, F.R. Two-equation eddy-viscosity turbulence models for engineering applications. *AIAA J.* **1994**, *32*, 1598–1605. [CrossRef]
34. Smagorinsky, J. General Circulation Experiments with the Primitive Equations. *Mon. Weather Rev.* **1963**, *91*, 99–164. [CrossRef]
35. Ivanov, N.G.; Zasimova, M.A. Mean air velocity correction for thermal comfort calculation: Assessment of velocity-to-speed conversion procedures using Large Eddy Simulation data. *J. Phys. Conf. Ser.* **2018**, *1135*, 012106. [CrossRef]
36. Ivanov, N.G.; Zasimova, M.A. Large Eddy Simulation of airflow in a test ventilated room. *J. Phys. Conf. Ser.* **2018**, *1038*, 012136. [CrossRef]
37. Zasimova, M.A.; Ivanov, N.G.; Markov, D. Numerical modeling of air distribution in a test room with 2D Sidewall JET. II. LES-computations for the room with finite width. *St. Petersburg State Polytech. Univ. J. Phys. Math.* **2020**, *13*, 75–92. [CrossRef]
38. Ivanov, N.; Zasimova, M.; Smirnov, E.; Markov, D. Evaluation of mean velocity and mean speed for test ventilated room from RANS and LES CFD modeling. *E3S Web Conf.* **2019**, *85*, 02004. [CrossRef]
39. Nicoud, F.; Ducros, F.; Nicoud, F.; Ducros, F. Subgrid-scale stress modelling based on the square of the velocity gradient tensor. *Turbul. Combust.* **1999**, *62*, 183–200. [CrossRef]
40. Courant, R.; Friedrichs, K.; Lewy, H. Uber die partiellen Differenzengleichungen der mathematischen Physik. *Math. Ann.* **1928**, *100*, 32–74. [CrossRef]
41. da Graça, G.C.; Albuquerque, D.P.; Sandberg, M.; Linden, P.F. Pumping ventilation of corner and single sided rooms with two openings. *Build. Environ.* **2021**, *205*, 108171. [CrossRef]
42. Thysen, J.H.; van Hooff, T.; Blocken, B.; van Heijst, G.J. Airplane cabin mixing ventilation with time-periodic supply: Contaminant mass fluxes and ventilation efficiency. *Indoor Air* **2022**, *32*, 13151. [CrossRef]
43. Holgate, J.; Skillen, A.; Craft, T.; Revell, A. A Review of Embedded Large Eddy Simulation for Internal Flows. *Arch. Comput. Methods Eng.* **2019**, *26*, 865–882. [CrossRef]

44. Sajjadi, H.; Ahmadi, G.; Delouei, A.A. Effect of Inlet Air Locations on Particle Concentration using Large Eddy Simulation based on Multi Relaxation Time Lattice Boltzmann Method. *J. Appl. Comput. Mech.* **2021**, *7*, 1944–1955. [CrossRef]
45. Zhang, Y.; Feng, G.; Bi, Y.; Cai, Y.; Zhang, Z.; Cao, G. Distribution of droplet aerosols generated by mouth coughing and nose breathing in an air-conditioned room. *Sustain. Cities Soc.* **2019**, *51*, 101721. [CrossRef]
46. Bazdidi-Tehrani, F.; Masoumi-Verki, S.; Gholamalipour, P. Impact of opening shape on airflow and pollutant dispersion in a wind-driven cross-ventilated model building: Large eddy simulation. *Sustain. Cities Soc.* **2020**, *61*, 102196. [CrossRef]
47. Xiao, X.; Zhou, J.; Yang, W. Review of calculating models of unsteady natural ventilation rate due to wind fluctuations. *Indoor Built Environ.* **2022**, *31*, 2199–2215. [CrossRef]
48. Dai, Y.; Mak, C.M.; Ai, Z. Flow and dispersion in coupled outdoor and indoor environments: Issue of Reynolds number independence. *Build Environ.* **2019**, *150*, 119–134. [CrossRef]
49. Arinami, Y.; Akabayashi, S.; Tominaga, Y.; Sakaguchi, J. Performance evaluation of single-sided natural ventilation for generic building using large-eddy simulations: Effect of guide vanes and adjacent obstacles. *Build. Environ.* **2019**, *154*, 68–80. [CrossRef]
50. Hwang, Y.; Gorlé, C. Large-eddy simulations to define building-specific similarity relationships for natural ventilation flow rates. *Flow* **2023**, *3*, E10. [CrossRef]
51. Jacob, J.; Merlier, L.; Marlow, F.; Sagaut, P. Lattice boltzmann method-based simulations of pollutant dispersion and urban physics. *Atmosphere* **2021**, *12*, 833. [CrossRef]
52. Adachi, Y.; Ikegaya, N.; Satonaka, H.; Hagishima, A. Numerical simulation for cross-ventilation flow of generic block sheltered by urban-like block array. *Build. Environ.* **2020**, *185*, 107174. [CrossRef]
53. Zhang, B.; Hu, H.; Kikumoto, H.; Ooka, R. Turbulence-induced ventilation of an isolated building: Ventilation route identification using spectral proper orthogonal decomposition. *Build. Environ.* **2022**, *223*, 109471. [CrossRef]
54. Hawendi, S.; Gao, S. Impact of windward inlet-opening positions on fluctuation characteristics of wind-driven natural cross ventilation in an isolated house using LES. *Int. J. Vent.* **2018**, *17*, 93–119. [CrossRef]
55. Laetitia, M.; Jiyun, S.; Alan, S.C.; Shuqin, C.; Jingdong, W.; Wei, Y.; Jie, X.; Qiulei, Z.; Jian, G.; Meng, L.; et al. The hot summer-cold winter region in China: Challenges in the low carbon adaptation of residential slab buildings to enhance comfort. *Energy Build.* **2020**, *223*, 110181. [CrossRef]
56. van Hooff, T.; Blocken, B.; Tominaga, Y. On the accuracy of CFD simulations of cross-ventilation flows for a generic isolated building: Comparison of RANS, LES and experiments. *Build. Environ.* **2017**, *114*, 148–165. [CrossRef]
57. Oksanen, L.; Auvinen, M.; Kuula, J.; Malmgren, R.; Romantschuk, M.; Hyvärinen, A.; Laitinen, S.; Maunula, L.; Sanmark, E.; Geneid, A.; et al. Combining Phi6 as a surrogate virus and computational large-eddy simulations to study airborne transmission of SARS-CoV-2 in a restaurant. *Indoor Air* **2022**, *32*, e13165. [CrossRef] [PubMed]
58. Vuorinen, V.; Aarnio, M.; Alava, M.; Alopaeus, V.; Atanasova, N.; Auvinen, M.; Balasubramanian, N.; Bordbar, H.; Erästö, P.; Grande, R.; et al. Modelling aerosol transport and virus exposure with numerical simulations in relation to SARS-CoV-2 transmission by inhalation indoors. *Saf. Sci.* **2020**, *130*, 104866. [CrossRef]
59. Busini, V.; Favrin, S.; Nano, G.; Derudi, M. Modelling of indoor air pollutants dispersion: New tools. *IOP Conf. Ser. Earth Environ. Sci.* **2018**, *167*, 012016. [CrossRef]
60. Liu, W.; van Hooff, T.; An, Y.; Hu, S.; Chen, C. Modeling transient particle transport in transient indoor airflow by fast fluid dynamics with the Markov chain method. *Build. Environ.* **2020**, *186*, 107323. [CrossRef]
61. Li, W.; Hasama, T.; Chong, A.; Hang, J.G.; Lasternas, B.; Lam, K.P.; Tham, K.W. Transient transmission of droplets and aerosols in a ventilation system with ceiling fans. *Build Environ.* **2023**, *230*, 109988. [CrossRef]
62. Zheng, M.; Fan, Y.; Li, X.; Lester, D.; Chen, X.; Li, Y.; Cole, I. Aerosol exchange between pressure-equilibrium rooms induced by door motion and human movement. *Build. Environ.* **2023**, *241*, 110486. [CrossRef]
63. Chu, C.R.; Su, Z.Y. Natural ventilation design for underground parking garages. *Build. Environ.* **2023**, *227*, 109784. [CrossRef]
64. Laitinen, A.; Korhonen, M.; Keskinen, K.; Kaario, O.; Vuorinen, V. Large-eddy simulation of buoyant airflow in an airborne pathogen transmission scenario. *Build Environ.* **2023**, *241*, 110462. [CrossRef]
65. Feng, G.; Bi, Y.; Zhang, Y.; Cai, Y.; Huang, K. Study on the motion law of aerosols produced by human respiration under the action of thermal plume of different intensities. *Sustain. Cities Soc.* **2020**, *54*, 101935. [CrossRef] [PubMed]
66. Bogdan, A.; Ogłodziński, K.; Szyłak-Szydłowski, M. Analysis of thermal plumes forming over male human subjects. *J. Build. Eng.* **2022**, *45*, 103596. [CrossRef]
67. Fang, X.; Yuen, A.C.Y.; Yeoh, G.H.; Lee, E.W.M.; Cheung, S.C.P. Numerical study on using vortex flow to improve smoke exhaust efficiency in large-scale atrium fires. *Indoor Built Environ.* **2023**, *32*, 98–115. [CrossRef]
68. Huang, Y.; Yeboah, S.; Shao, J. Numerical investigation of fire in the cavity of naturally ventilated double skin façade with venetian blinds. *Build. Serv. Eng. Res. Technol.* **2023**, *44*, 45–61. [CrossRef]
69. Larkermani, E.; Cao, G.; Georges, L. Characterization of the density-driven counter-flow through a doorway using Large Eddy Simulation. *Build. Environ.* **2022**, *221*, 109319. [CrossRef]
70. Zong, J.; Ai, Z.; Ma, G. Accurate evaluation of inhalation exposure based on CFD predicted concentration in the breathing zone towards personalized and smart control. *J. Build. Eng.* **2023**, *71*, 106404. [CrossRef]
71. Lordly, K.; Kober, L.; Jadidi, M.; Antoun, S.; Dworkin, S.B.; Karataş, A.E. Understanding lifetime and dispersion of cough-emitted droplets in air. *Indoor Built Environ.* **2022**. [CrossRef]

72. Jiang, J.; Jiang, Z.; Kwan, T.H.; Liu, C.H.; Yao, Q. Study of indoor ventilation based on large-scale DNS by a domain decomposition method. *Symmetry* **2019**, *11*, 1416. [CrossRef]
73. Hoque, S.; Omar, F.B. Coupling Computational Fluid Dynamics Simulations and Statistical Moments for Designing Healthy Indoor Spaces. *Int. J. Environ. Res. Public Health* **2019**, *16*, 800. [CrossRef] [PubMed]